Carbohydrate Polymers 108 (2014) 176–182

Contents lists available at ScienceDirect

Carbohydrate Polymers

journal homepage: www.elsevier.com/locate/carbpol

Wet spinning of fibers made of chitosan and chitin nanofibrils

Vladimir E. Yudin[a,b], Irina P. Dobrovolskaya[a,*], Igor M. Neelov[a,c], Elena N. Dresvyanina[a], Pavel V. Popryadukhin[a], Elena M. Ivan'kova[a], Vladimir Yu. Elokhovskii[a], Igor A. Kasatkin[d], Boris M. Okrugin[d], Pierfrancesco Morganti[e]

[a] Institute of Macromolecular Compounds Russian Academy of Sciences, 31 Bolshoy pr. VO, Saint-Petersburg, 199004 Russia
[b] Saint-Petersburg Polytechnic University, Polytechnicheskaya ul. 29, Saint-Petersburg, 195251 Russia
[c] Saint-Petersburg National Research University of Information Technologies, Mechanics and Optics, Kronverkskiy pr., 49, Saint-Petersburg, 197101 Russia
[d] Saint-Petersburg State University, Universitetskaya nab.7-9, Saint-Petersburg, 199034 Russia
[e] Applied Cosmetic Dermatology, II University of Naples, Italy

ARTICLE INFO

Article history:
Received 9 December 2013
Received in revised form 21 February 2014
Accepted 27 February 2014
Available online 12 March 2014

Keywords:
Chitin/chitosan
Composite fibers
Structure
Modeling

ABSTRACT

Biocompatible and bioresorbable composite fibers consisting of chitosan filled with anisotropic chitin nanofibrils with the length of 600–800 nm and cross section of about 11–12 nm as revealed by SEM and XRD were prepared by coagulation. Both chitin and chitosan components of the composite fibers displayed preferred orientations. Orientation of chitosan molecules induced by chitin nanocrystallites was confirmed by molecular modeling. The incorporation of 0.1–0.3 wt.% of chitin nanofibrils into chitosan matrix led to an increase in strength and Young modulus of the composite fibers.

1. Introduction

Recently the films, fibers and porous bulk materials based on the natural polysaccharide chitin are used as the matrices for biomedical applications (Pillai, Paul, & Sharma, 2009; Rathke & Hudson, 1994; Sriupayo, Supaphol, & Rujiravanit, 2005). During processing of the polymer dimethylacetamide containing LiCl is used as a solvent, the residual ions from which are hard to remove from the polymer after processing. This decreases biocompatibility of the material and increases its cytotoxicity.

Chitosan – the N-deacetylated derivative of chitin (Muzzarelli, 1983; Panarin, Nud'ga, Petrova, & Bochek, 2009) is the most promising polymer which combines bioresorption, absence of cytotoxicity and low environmental impact during processing. However, due to its highly hydrophilic nature, the properties of materials based on chitosan are unstable and their strength and rigidity are reduced in the wet state. To optimize mechanical properties of chitosan-based materials chitin nanoparticles (Sriupayo et al., 2005) or inorganic chrysotile nanotubes (Dobrovol'skaya, Popryadukhin, Khomenko, Dresvyanina, & Yudin, 2011) can be loaded into the chitosan matrix. A study of structure and properties of composite fibers showed that incorporation of 1–3 wt.% chrysotile nanotubes into the chitosan matrix induces preferred orientation of the chitosan fibers, increases their strength and Young modulus. However, the chrysotile nanotubes are resistant to biodecomposition, and they can remain in the living organism for a very long time. Composite fibers characterized by good bioresorption properties of both the matrix and the filler can therefore be developed and used as one-dimensional matrices for the cellular technologies. Recently, organic nanoparticles were prepared on the basis of chitin, chitosan and cellulose (Abe, Iwamoto, & Yano, 2008; Fan, Saito, & Isogai, 2008; Muzzarelli et al., 2007; Shinsuke et al., 2010). The introduction the chitin nanofibrils into the chitosan matrix makes it possible to form the bioresorbable composite fibers, which are characterized by the increased strength and elastic characteristics. In this work we report our progress in preparation of chitosan fibers filled by the chitin nanofibrils and study of their structure and mechanical properties.

2. Experimental

The chitin nanofibrils (Mavi Sud s.r.l, Italy) and the chitosan (Fluka Chemie, Bio Chemika line) were used for preparing the

* Corresponding author. Tel.: +7 812 323 5065.
E-mail address: dobrov@hq.macro.ru (I.P. Dobrovolskaya).

http://dx.doi.org/10.1016/j.carbpol.2014.02.090
0144-8617/

composite fibers. The degree of deacetylation of chitosan was 83%, molecular weight M_w = 215 kDA.

The suspension of the chitin nanofibrils in the water was homogenized with the aid of an ultrasonic mixer (40 kHz, average sonic power 45 W) for 30 min. A mixture of the chitosan solution with the chitin nanofibrils was prepared by adding a desired amount of the chitosan powder to chitin water suspension to obtain a 4 wt.% solution. The concentration of the chitin nanofibrils with respect to dry chitosan varied in the range of 0.05–20 wt.%. The mixtures (pH = 4–5) were stirred at RT for 30 min until the partial dissolution of chitosan and its swelling. Then the 2% acetic acid solution in water was introduced into the mixture during a continuous stirring. The mixture of the solution of chitosan with the chitin nanofibrils was stirred in the glass bulb at RT during 90 min, and then it was filtered and deaerated for 24 h at the pressure 0.1 atm.

The fibers were prepared by a coagulation method (Hiroshi et al., 2004) using a laboratory equipment developed at the Institute of Macromolecular Compounds RAS. The 1:1 mixture of 10% solutions of NaOH and C_2H_5OH was used as a precipitator. The solution was fed through the die hole with the diameter of 0.6 mm with the rate of 5.5 mm/s; the time of precipitation was 150 s. The factor of orientation drawing (λ) of the monofilament in the coagulation bath was varied from −40% (shrinkage) up to +120%. The fibers were washed in the distilled water and then dried at 50 °C during 10 min.

Rheological measurements of polymer solutions were conducted with the rheometer Physica MCR 301 (Anton Paar) at 20 °C by the "cylinder in the cylinder" method in the regime of shear flow with the shear rates 10^{-4}–10^{2} s^{-1}. 5 mL of solution was placed into the rheological cuvette and the dependence of viscosity (η) on the shear rate ($\dot{\gamma}$) was obtained.

The scanning electron microscopy (SEM, Supra-55 VP, Carl Zeiss) and X-ray diffraction (WAXD, Bruker D8 DISCOVER) were used for studying the fine structure of the composite fibers.

The measurements of the mechanical properties of the processed fibers were carried out on the testing machine UMIV (Russia) at RT and the load speed of 1 mm/min; basis length of the fibers was 15 mm. The cross sections (S in m^2) of the monofilaments were estimated by the formula $S = \text{tex}/\rho$, where tex is the mass of 1 m of monofilament and specific gravity (ρ) of chitosan was equal to 1400 kg/m^3. Prior to the mechanical testing the fibers were kept at relative air humidity of 66% for 24 h.

To understand the molecular mechanism of orientation of chitosan molecules induced by chitin nanoparticles we performed energy minimization and molecular dynamics simulation of the systems containing a single chitosan molecule on the surface of chitin nanocrystallite. OPLS and AMBER94 force fields were used in these calculations. In our simulations the chitin nanocrystallite consisted of 16 chitin chains (four chains in each of the four layers) each composed of 8 monomers. The initial conformations of these chitin chains were taken from crystal structure of α-chitin obtained in both an experiment and a recent DFT simulation (Petrov, Lymperakis, Friak, & Neugebauer, 2013). Single chitosan chain (with degree of deacetylation of 75%) was also composed of 8 monomers to make its length close to the size of chitin nanocrystallite.

3. Results and discussion

3.1. Structure of the chitin nanofibrils

To obtain a composite material on the basis of a polymer matrix filled with nanoparticles of various shapes a uniform particle distribution should be achieved. The dispersion of nanoparticles depends on the nature of interaction between the polymer and the filler, which is in turn determined by the special features of their chemical and supermolecular structure. Therefore, special attention in the present work was given to the study of the chitin nanofibril structure. Chitin is natural aminopolysacharide containing the lateral group —NH—CO—CH_3; it occurs in two polymorphic forms. In the first modification the chitin macromolecules are packed in antiparallel orientation (α-chitin), and in the second one they are parallel (β-chitin). Both structural modifications can co-exist in a living organism (Sikorski, Hori, & Wada, 2009).

The method of obtaining the chitin particles consists in the lyophilization of the initial chitin suspension. As a result, the powder consisting of the microparticles was obtained. Fig. 1 represents the SEM micrographs of the material taken at different magnifications. It is evident that the microparticles have a strip morphology with the characteristic width of about 30 μm and the thickness of 0.1 μm (Fig. 1a); they consist of nanofibrils with the width of 20 nm and the length in the range of 600–800 nm (Fig. 1b).

The X-ray diffraction pattern of the chitin powder obtained by lyophilization is shown in Fig. 2. The presence of intensive diffraction peaks testifies the crystal structure of α-chitin with the following unit cell parameters: a = 0.473 nm, b = 1.899 nm, c = 1.025 nm which agree well with the literature data (Sikorski et al., 2009). The unit cell parameter b is substantially greater than the a which is, apparently, caused by the presence of the lateral group —NH—CO—CH_3 in the macromolecule. The macromolecules in the unit cell of this crystalline modification are located antiparallel to each other. An average crystallite size was estimated in two ways: (1) using integral breadth ("Laue width") of all detected diffraction peaks; (2) using angular full width at half-maximum (FWHM) of individual peaks (Sherrer's method). The average crystallite size determined by the first way was L = 12.5 nm. The estimation of the crystallite size in the direction of b-axis according to the Sherrer's method for the 020 peak resulted in the value of L = 11.1 nm. To estimate the crystallite size in the direction of c-axis (i.e. in the direction of the of macromolecules axis) was impossible in view of the absence of clearly resolved 0 0 2 peak or its higher orders. This might indicate a substantially smaller size of crystallites in the direction of macromolecule axis and/or their pronounced defectiveness.

The comparison of the data from X-ray diffraction analysis with the results of SEM examinations makes it possible to conclude the following: (1) along its width each individual chitin nanofibril consists of about two crystallites with transverse sizes of 11–12 nm, whose b-axes are located perpendicularly to the nanofibril axis (see Fig. 2); (2) the inner crystallite structure of the individual chitin nanofibril is better ordered in the transversal direction than in the longitudinal one. On the contrary, the longitudinal crystallite size of the cellulose and its derivatives in the oriented state is usually larger than the transverse one and equals approximately to 7 nm (Dobrovolskaya, Slutsker, Chereisky, & Utevsky, 1975).

3.2. Rheology of the polymer solution

The chitin nanofibrils were used as a filler for obtaining the bioresorbable composite fibers. To optimize the regime of wet spinning the information about the rheological properties of the chitosan solution and its mixtures with the filler is necessary. Fig. 3 represents the dependences of the viscosity on the shear rate for the chitosan solution and its mixtures with chitin nanofibrils. The content of chitin nanofibrils with respect to the dry chitosan varied from 0.05 to 20 wt.%.

As seen in Fig. 3 the dependencies of the viscosity (η) on the shear rate ($\dot{\gamma}$) for all investigated solutions have a nonlinear behavior. In the chitosan solution without filler, the decrease of viscosity was observed at the shear rate of 10 s^{-1} or more. The threshold value of the shear rate at which the dependence $\eta(\dot{\gamma})$ becomes nonlinear shifts to the smaller values with increasing content of

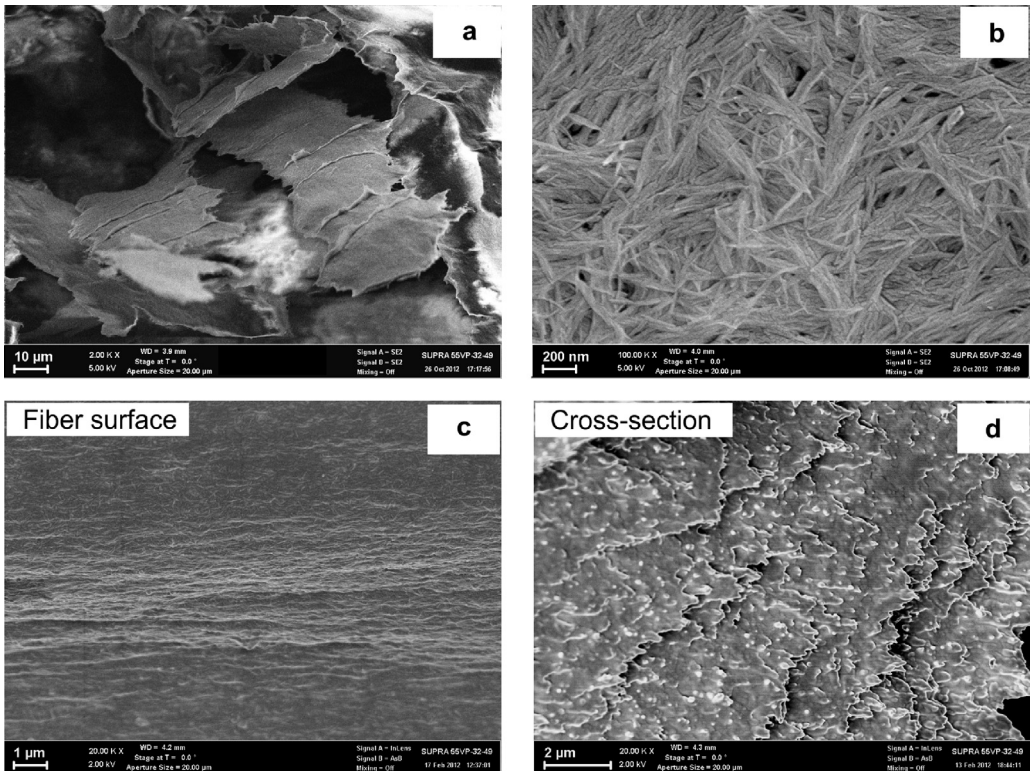

Fig. 1. Scanning electron micrographs of the film obtained from chitin nanofibril water dispersion by freeze drying (a and b); cross section of the composite monofilament chipped in a liquid nitrogen, fiber contains 1 wt.% of chitin nanofibrils (c and d).

chitin nanofibrils. For the mixture containing 20 wt.% of chitin filler the dependence of $\eta(\dot{\gamma})$ becomes linear over a wide range of shear rates. Generally, the decrease in viscosity upon an increase in the shear rate is related to the destruction of the initial structure of the polymer solution and the creation of a new oriented structure that means transition from isotropic state to anisotropic one. The formation of the anisotropic structure of the polymer solution under the action of shear field is typical of the majority of rigid-chain polymers (Garboczi, Snyder, Douglas, & Thorpe, 1995).

An increase in the chitin nanofibril content in the chitosan solution is accompanied by an increase in the viscosity, which is especially noticeable at the low shear rates. This indicates good interaction of the chitin nanofibrils with chitosan macromolecules and the formation of the cluster structure of the filler when the chitin nanofibril concentration is larger than 1 wt.% (with respect to the dry chitosan). The dependences of $\eta(\dot{\gamma})$ for the mixtures containing 0.1, 0.3, 0.5, 0.7 wt.% chitin nanofibrils practically coincide with that of pure chitosan solution. Thus, processing of composite chitosan/chitin fiber wet spinning at very low chitin nanofiblil content (<1%) should be close to processing of pure chitosan fibers.

3.3. Structure and properties of the chitosan/chitin composite fibers

It is shown in (Dobrovol'skaya et al., 2011; Dresvyanina, Dobrovolskaya, Popryadukhin, Yudin, & Ivan'kova, 2012) that the

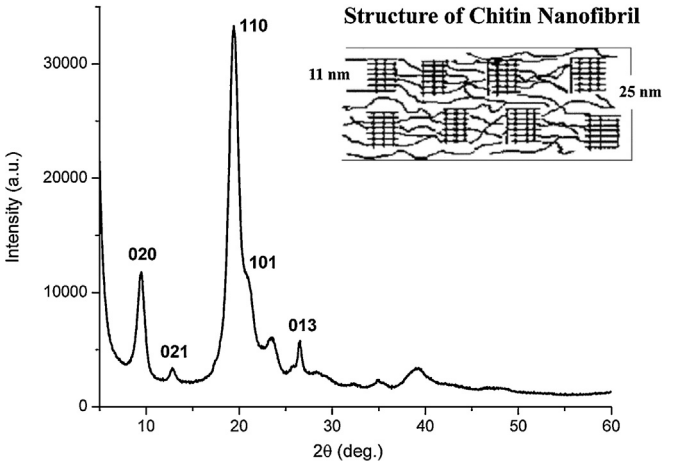

Fig. 2. X-ray diffraction pattern of the chitin nanofibril powder obtained by lyophilization of its water dispersion.

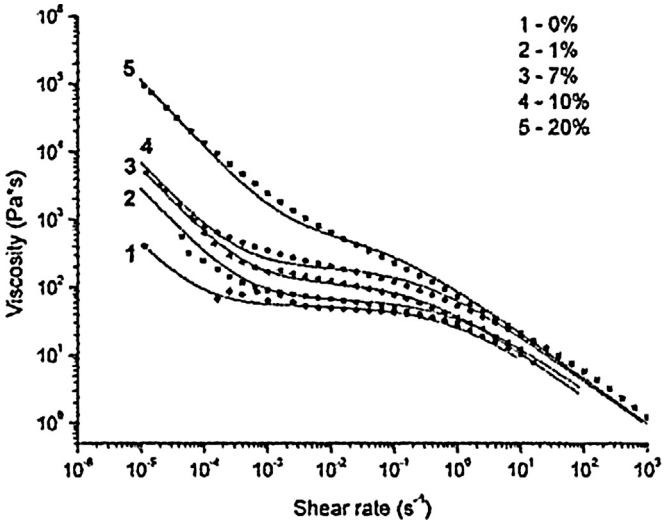

Fig. 3. Dependences of viscosity on shear rate for chitosan solution with different concentrations of chitin nanofibrils.

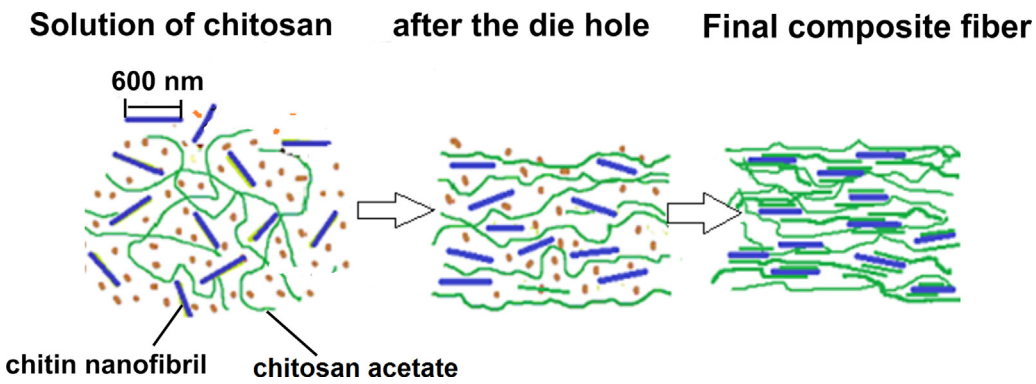

Fig. 4. Formation of the chitosan (green) composite fiber structure containing chitin nanofibrils (blue) (For interpretation of the references to color in this figure legend, the reader is referred to the web version of this article.).

oriented structure of the chitosan fibers is formed during flowing of the solution (or its mixture with the nanoparticles) through the die hole. In turn, the orientation of the nanoparticles and the macromolecules depends on the shear stress occurring in the die hole. The optimum rate Q (mL/min) of the polymer solution through the die hole of the radius R can be calculated according to the proportion $Q = \pi\dot{\gamma}R^3/2$ which is correct for Newtonian liquids (Baird, 1978). The shear rate $\dot{\gamma}$ should be quite high in order to provide good orientation of the macromolecules but not too high in order to make possible the complete coagulation of the fiber in the alkali/ethanol bath. Thus, keeping in mind these two criteria, the Q has been chosen to about 0.1 mL/min. This value corresponded approximately to the $\dot{\gamma} \sim 10^{-1}$ s^{-1} as indicated in Fig. 3.

It turned out that the chitosan solutions containing chitin nanofibrils possessed the necessary dynamic properties allowing to preserve the laminarity of the jet in the coagulation bath after the flowing of the solution through the die hole. Therefore, the spinning of the pure chitosan and composite chitosan/chitin monofilaments was carried out by coagulation method with the identical rates Q and the different factors of orientation drawing λ.

It follows from the results of SEM examination that the monofilaments on the basis of chitosan have smooth surface and homogeneous internal structure as do the majority of the fibers obtained by similar method. The special feature of the chitosan/chitin fiber morphology is the presence of flat fibril-like structures, that are distinctly visible (Fig. 1c and d) in the cross section of the monofilament obtained after its fracture in a liquid nitrogen.

The flat fibril-like structures include the chitin nanofibrils, (width about 25–30 nm) oriented along the fiber axis. This value is somewhat larger than the size determined for the freeze-dried suspension of chitin nanofibrils (20 nm), that suggests a good adhesion of chitosan to chitin nanofibril or existence of thin (~5–10 nm) chitosan layer on the chitin nanofibril surface. A good adhesion of chitosan to chitin nanofibrils is caused by the fact that chitosan macromolecules contain lateral groups of both NH_2 and —NH—CO—CH_3, the latter are characteristic of the chitin macromolecules as well.

The chitosan fiber was obtained under the equilibrium conditions when the monofilament is not affected by the tensile stresses after its exit from the die hole. As a result, this chitosan fiber after processing in the coagulation bath displayed a shrinkage of about $\lambda = -40\%$. The azimuthal distribution of the intensity within the 200 and 220 Debye diffraction rings reveals no strong texture maxima and suggests a practically isotropic structure of the chitosan fiber. The drawing of the fiber ($\lambda = 60\%$) during its processing leads to strengthening the preferred crystallite orientation. This is manifested in the appearance of the texture maxima at the equator of the X-ray diffraction pattern. It should be noted that the distribution of the intensity in the arc form is observed for the majority of the investigated chitosan fibers and composite fibers containing the chitin nanofibrils. Even the small drawing of all these fibers leads to the chitosan crystallite orientation. Formation process of the structure of composite fibers based on chitosan and chitin nanofibrils is shown schematically in Fig. 4.

The presence of two wide diffraction peaks leads to the conclusion that chitosan and chitosan/chitin fibers are characterized by a defect-rich crystal structure, shifts and rotary disturbances of three-dimensional order. The reason of this effect can be the presence of both “chitosan” and “chitin” fragments in the polymer chain that prevents crystallization. The ordering of crystalline regions does not depend practically on the degree of fiber drawing nor on the quantity of chitin nanofibrils in the fibers (up to the 10%). The higher content of chitin nanofibrils (20%) leads to the appearance of the 0 2 0 reflex ($2\theta \approx 9^\circ$) of chitin at the diffractogram of chitosan/chitin fibers and a change in the profile of the maximum at the angle of $2\theta \approx 20^\circ$, which is connected with the overlapping of the chitosan and chitin reflexes.

The dependences of the strength of chitosan and composite chitosan/chitin fibers on the factor of orientation drawing (λ) are given in Fig. 5. From the preceding data it is evident that the strength of the chitosan fibers (without filler) grows considerably with an increase in the drawing up to $\lambda \sim 20\%$.

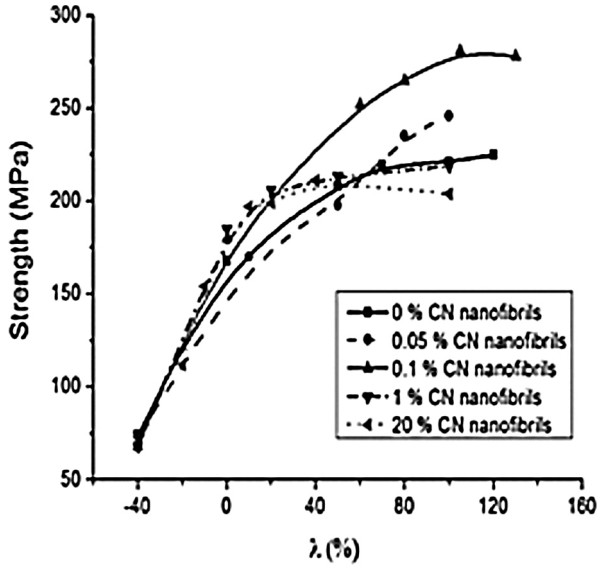

Fig. 5. Dependences of the tensile strength of chitosan and chitosan/chitin composite fibers on the factor of orientation drawing λ for different chitin (CN) nanofibril content.

Table 1
The azimuthal distribution intensity FWHM (φ) of the chitosan/chitin composite fibers processed with different factor of orientation drawing λ.

Chitin nanofibrils content, wt.%	Orientation drawing, λ, %	φ, degree
0	−40	90.6
	0	29.5
	30	31.2
	60	29.4
0.1	−40	57.2
	0	29.1
	23	27.6
	90	29.5
1	−40	62.4
	0	28.8
	66	30.0
	90	30.6
	180	28.3
20	20	32.7

Further drawing does not affect the fibers strengthening. The strength of the composite chitosan/chitin fibers containing a small quantity (0.05–0.3 wt.%) of the filler increases monotonically with the drawing up to λ ~ 120%. An increase in the content of chitin nanofibrils in the composite fibers above 1 wt.% significantly changes the nature of the $\sigma(\lambda)$ dependence. An increase in the strength ceases at λ ~ 20% just as it does in the case of the unfilled chitosan fibers. This is connected with the difficulties of the processing of these fibers due to an increase in the solution viscosity (see Fig. 3).

Increasing the viscosity of a chitosan solution containing the chitin nanofibrils may be explained by the formation of cluster structure of the filler. Percolation threshold R_p (vol%) is possible to estimate theoretically (Garboczi et al., 1995) by using the equation for a cylinder: $R_p = (0.6/r)$ 100%, where the aspect ratio $r = L/d$, and L is the length and d is the diameter of the cylinder. According to SEM and X-ray diffraction, $L \sim 800$ nm and $d \sim 20$ nm in the chitin nanofibrils. Thus, according to these experimental data the values of $r \sim 40$ and $R_p \sim 1.5$ vol.% were calculated. When concentrations of chitin nanofbrils are higher than this percolation threshold, the structural network can be formed. This prevents the orientational drawing of the composite fibers. In view of the similar values of the specific gravitiy ~1400 kg/m^3 of chitosan and chitin it is possible to conclude that the percolation threshold of chitin nanofibrils in the chitosan matrix is about 1.5 wt.%.

An increase in the fiber strength is caused by a change in their morphology and by orientation of the macromolecules. The chitosan crystallite orientation during wet spinning of the fibers was evaluated according to FWHM (φ) of the azimuthal distribution of the diffraction peak intensity.

From the data given in Table 1 it follows that even small drawing leads to the essential orientation of the crystallites. The value φ depends on the chitin nanofibril content. A small quantity of the filler contributes to the orientational drawing of fibers: The maximum orientation of crystallites is observed already at λ ~ 0%. Further increase in λ does not contribute significantly to the orientation of crystallites. At the same time, strength and Young modulus of fibers increases considerably. This can be explained probably by the orientation of macromolecules in the intercrystalline regions of the chitosan microfibrils.

The chitosan/chitin composite fibers spun under the equilibrium conditions (λ = −40%) display a sharper texture than the chitosan fibers containing no filler (Table 1). Introduction of 1 wt.% chitin nanofibrils makes it possible to obtain the oriented crystallite structure (compare $\varphi = 90.6^\circ$ and $\varphi = 62.4^\circ$) without any drawing of the monofilament during its processing. This allows one to assume that the presence of the chitin nanofibrils itself promotes the orientation of chitosan macromolecules. Actually, as can be seen from SEM micrograph (Fig. 1d) the chitin nanofibrils are well oriented along the fiber axis. The shift stresses appearing during the flow of the chitosan solution with chitin nanofibrils through the die hole facilitate this orientation.

The orientation of the chitin nanofibrils and their strong interaction with the chitosan matrix increase the strength and elastic characteristics of the chitosan/chitin composite fibers. The dependencies of the strength and Young modulus of the chitosan/chitin fibers on the content of chitin nanofibrils are illustrated in Fig. 6. These dependences have non-monotonic character; the maximum values of the fiber strength and the modulus occur at about 0.3 wt.% chitin concentration. Really, the optimum content of the filler of 0.1–0.3 wt.% ensures the additional orientation of the chitosan macromolecules on the chitin nanofibril surface on the one hand, and on the other hand - a sufficient mobility of the chitosan macromolecules for their orientation during fiber drawing. When the concentration of the chitin nanofibrils increases up to R_p or higher the formation of rigid network from the particles (cluster structure) occurs that leads to the reduction of the chitosan macromolecule mobility. The chitosan macromolecule orientation processes in the composite fibers with a cluster structure are hindered. This may explain the decrease in strength and Young modulus of the fibers, which contain more than 0.3 wt.% of the chitin nanofibrils. This value (0.3 wt.%), which is less than 1.5 wt.% (percolation threshold) for chitin nanofibril concentration, can be explained probably by the filler agglomeration and by some problems with the fiber processing due to increase in chitosan/chitin solution viscosity. Nevertheless, the increase in the strength (1.4 times) and Young modulus (1.5 times) of the chitosan fibers at small chitin concentrations (0.3 wt.%) cannot be explained by a reinforcing effect of chitin nanofibrils. This is more

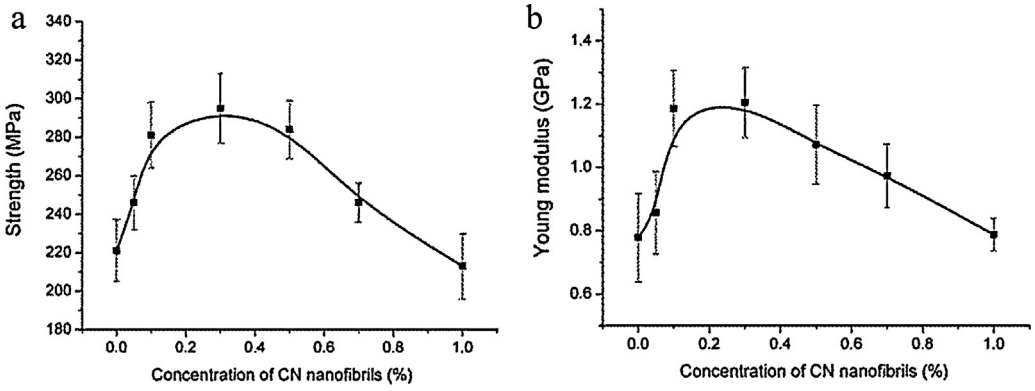

Fig. 6. Dependences of tensile strength (a) and Young modulus (b) of the chitosan/chitin composite fibers on the content of the chitin nanofibrils.

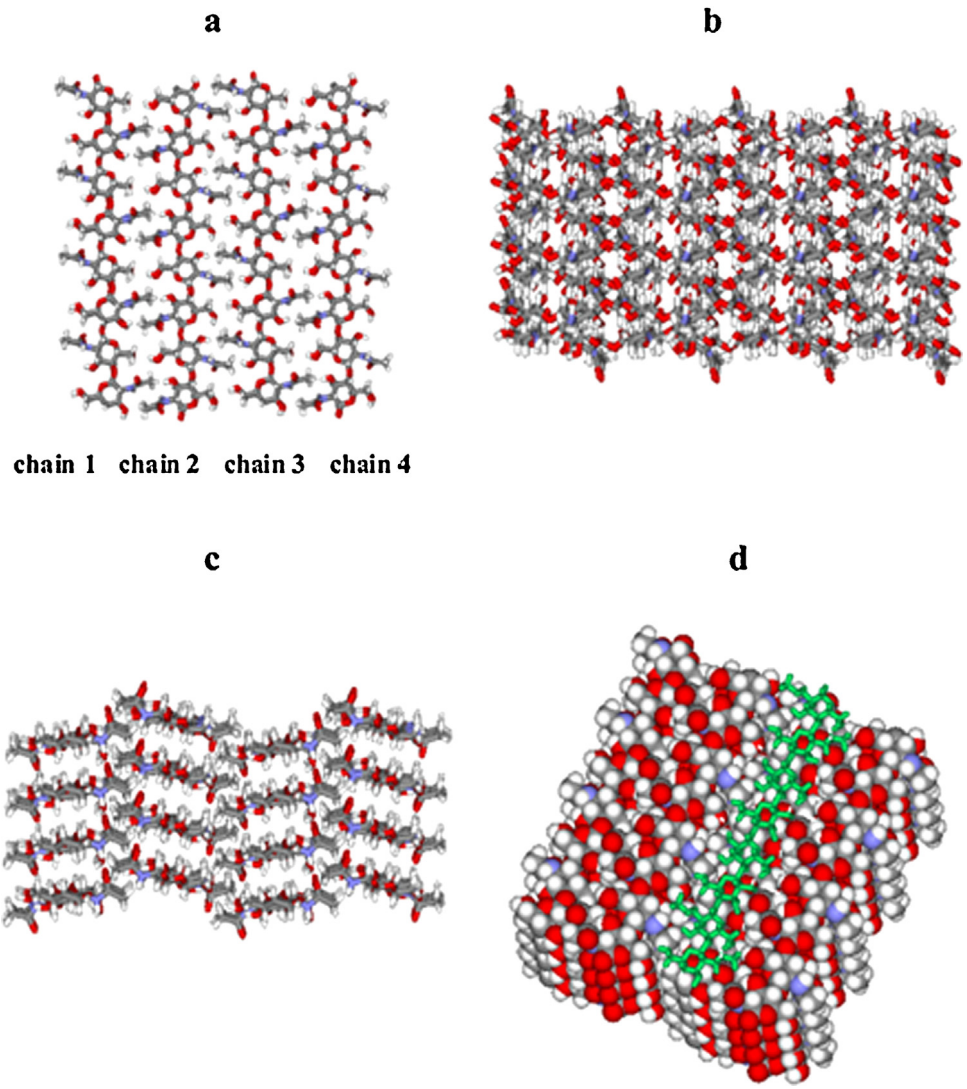

Fig. 7. Chitin nanocrystallite consisting of 16 chain 8 monomer each: (a) view from above; (b and c) side view (surface layer of the crystallite consists of 4 chitin chains (chain 1–chain 4); (d) one chitosan chain (green) on surface of the chitin crystallite. Position and orientation of the chitosan chain in contact with the "chain 3" of the crystallite surface (see Fig. 7a and d) corresponds to the lowest energy of interaction E_{int} in Table 2. Carbon atoms – gray, oxygen – red, nitrogen – blue and hydrogen – white. (For interpretation of the references to color in this figure legend, the reader is referred to the web version of this article.)

probably connected with the more effective orientation of the chitosan macromolecules in the presence of chitin as compared with unfilled polymer.

The process of the orientational drawing of the chitosan/chitin composite fibers with the low (<1 wt.%) content of filler can be described by the following model. The chitin nanofibrils are located chaotically in the solution and the preferred orientation is absent. There is a sufficiently large volume between chitin nanofibrils, in which chitosan macromolecules are located. The orientation of both chitin nanofibrils and chitosan macromolecules during fiber processing occurs in the field of shear stresses, especially when the polymer solution flows through the die hole. Due to a good adhesion, the chitosan macromolecules located in the near-surface layer of the chitin nanofibrils acquire additional orientation. During the drawing process in the coagulation bath the orientation of the chitosan macromolecules occurs, that leads to the formation of the oriented crystal structure of chitosan. Further increase in the drawing contributes to the orientation of the chitosan macromolecules in the intercrystalline amorphous regions inside the chitosan microfibrils.

3.4. Orientation of chitosan molecules by chitin nanoparticles. Molecular modeling

Different orientations and positions of a chitosan chain with respect to the four surface chitin chains were studied (Fig. 7). In particular, the angles of initial orientations of chitosan chain relative to the chitin chains were taken from 0° to 180° where the angle 0° corresponds to the orientation of chitosan chains parallel to backbones of the chitin chains in a crystallite. For the chitosan chain with orientation angle equal to 0° we also checked several initial positions of chitosan chain on the surface which were obtained by shifting the chain along the surface in the direction perpendicular to the chain backbone (4 positions of the single chitosan chain on the surface exactly above each of the 4 surface chitin chains, and 3 positions of the chitosan chain on the surface exactly between each pair of these 4 chitin chains (see Fig. 7)). We carried out energy minimization of these systems and then short molecular dynamics (MD) simulations, took several low energy conformations from each MD simulation and did a second minimization to get the lowest energy conformations for each system. The results are presented in Table 2.

Table 2
Energy E_{int} per monomer for interaction between a single chitosan molecule and a surface of chitin crystallite at different orientations and positions of the chain on the surface. (Positions 1–4 of the chitosan chain are exactly above the positions 1–4 of the chitin chains in the surface layer of the crystallite (see Fig. 7). Results of the energy minimization with OPLS and AMBER94 force fields are shown as E_{int}^{OPLS} and $E_{int}^{AMBER94)}$.

N	Orientation, grad, (position of chain)	E_{int} OPLS (kcal/mol)	E_{int} AMBER94 (kcal/mol)
0	0 (3rd)	−13.53	−13.16
1	15	−4.96	−4.99
2	30	−4.91	−4.68
3	45	−4.48	−4.54
4	90	−4.93	−4.73
5	180	−8.97	−8.33
6	120	−5.13	−4.97
7	135	−6.64	−6,01
8	150	−5.96	−5.65
9	0 (1st)	−11.34	−7.55
10	0 (2nd)	−10.26	−6.02
11	0 (4th)	−9.99	−9.36
12	0 (between 1st & 2nd)	−6.30	−5.79
13	0 (between 2nd & 3rd)	−9.47	−8.87
14	0 (between 3rd & 4th)	−8.24	−8.06

It is easy to see that for most of the conformations the results of OPLS and AMBER94 force fields are close to each other. A chitosan molecule oriented non-parallel to chitin molecules (lines 1–4 and 6–8 in Table 2) has a weak interaction with the surface of a chitin crystallite (value E_{int} for the most of these conformations are between −4 and −6 kcal/mol). At the same time the chitosan chains parallel or antiparallel to chitin molecules (lines 0.5 and 9–14 in Table 2) have stronger interaction energy values (E_{int} = −6 to −11 kcal/mol for most of them). For the chitosan chains parallel to the chitin chains the strongest interaction energies are found for the position of the chain above the odd (1st and 3rd) chitin chains in Fig. 7a, corresponding to the lines 9 and 0 of Table 2, with the absolute minimum of energy for the line 0 (E_{int} = −13.53 for OPLS and −13.16 for AMBER94 force fields).

A chitosan chain in this position has the strongest attraction to the chitin surface which is stronger by 2–9 kcal/mol than the interaction of this chain in a non-parallel orientation. This result is in line with the experimental results showing that the chitosan chains are oriented by the chitin nanofibrils.

4. Conclusions

The composite chitosan fibers filled with the chitin nanofibrils are prepared from an aqueous solution of 2% acetic acid by coagulation method. It is shown that the nonlinear character of the dependence of the chitosan/chitin solution viscosity on the shear rate is caused by the orientation of the chitosan macromolecules and chitin nanofibrils that is confirmed by the data of the scanning electron microscopy and the X-ray diffraction analysis. Individual chitin nanofibrils is found to consist of two 11–12 nm crystallites in the transverse direction; the *b*-axes are located perpendicularly to the axis of the nanofibril.

The introduction of the chitin nanofibrils in the quantity of 0.1–0.3 wt.% in the chitosan matrix contributes to the orientation of the chitosan macromolecules that leads to an increase in the strength and Young modulus of the chitosan/chitin composite fibers. The orientation of the chitosan macromolecules on the surface of the CN nanofibrils is confirmed by the energy minimization and molecular dynamics simulation of systems containing one chitosan molecule on the chitin nanocrystallite surface

Acknowledgments

Financial support of this work by the Russian Foundation for Basic Research under contract grants #13-03-00748 and # 12-03-31483 is gratefully acknowledged.

XRD studies have been performed at the Research Centre for X-ray Diffraction Studies, St. Petersburg State University.

References

Abe, K., Iwamoto, H., & Yano, H. (2008). Obtaining cellulose nanofibrils with a uniform width of 15 nm from wood. *Biomacromolecules*, *8*, 3276–3278.

Baird, D. G. (1978). Viscometry of anisotropic solutions of poly-p-phenyleneterephthalamide in sulfuric acid. *Journal of Applied Polymer Science*, *22*, 2701–2706.

Dobrovol'skaya, I. P., Popryadukhin, P. V., Khomenko, A. Yu., Dresvyanina, E. N., Yudin, V. E., Elokhovskii, V. Yu., et al. (2011). Structure and characteristics of chitosan based fibers containing chrysotile and halloysite. *Polymer Science Series A*, *53*, 418–423.

Dobrovolskaya, I. P., Slutsker, L. I., Chereisky, Z. Yu., & Utevsky, L. E. (1975). Changing the structure of rayon fibers during pyrolysis. *Polymer Science USSR Seriya A*, *17*, 1555–1559.

Dresvyanina, E. N., Dobrovolskaya, I. P., Popryadukhin, P. V., Yudin, V. E., & Ivan'kova, E. M. (2012). Influence of spinning conditions on properties of chitosan fibers. *Fiber Chemistry*, *44*, 260–263.

Fan, Y., Saito, T., & Isogai, A. (2008). Chitin nanocrystals prepared by TEMPO-mediated oxidation of α-chitin. *Biomacromolecules*, *9*, 192–198.

Garboczi, E., Snyder, K., Douglas, J., & Thorpe, M. (1995). Geometrical percolation threshold of overlapping ellipsoids. *Physical Review*, *52*, 819–828.

Hiroshi, T., Yukihiko, T., Kouki, I., Wannasiri, W., Ratana, R., & Seiichi, T. (2004). Preparation of chitosan filament applying new coagulation system. *Carbohydrate Polymers*, *56*(2), 205–211.

Muzzarelli, R. A. A. (1983). Chitin and its derivatives: New trends of applied research. *Carbohydrate Polymers*, *3*(4), 53–75.

Muzzarelli, R. A. A., Morganti, P., Morganti, G., Palombo, P., Palombo, M., Biagini, G., et al. (2007). Chitin nanofibrils/chitosan glycolate composites as wound medicaments. *Carbohydrate Polymers*, *70*(3), 274–284.

Panarin, E. F., Nud'ga, L. A., Petrova, V. A., & Bochek, A. M. (2009). Composite chitin and chitosan based matrices for culturing human dermal cells. *Cellular Transplantation and Tissue Engineering*, *4*, 42–46.

Petrov, M., Lymperakis, L., Friak, M., & Neugebauer, J. (2013). Ab initio based conformational study of the crystalline α-chitin. *Biopolymers*, *99*, 22–34.

Pillai, C. K. S., Paul, W., & Sharma, C. P. (2009). Chitin and chitosan polymers: Chemistry, solubility and fiber formation. *Progress in Polymer Science*, *34*, 641–678.

Rathke, T. D., & Hudson, S. M. (1994). Review of chitin and chitosan as fiber and film formers. *Journal of Macromolecular Science*, *34*, 375–437.

Shinsuke, I., Masaya, N., Masafumi, Yo., Minoru, M., Hiroyuki, Ya., & Hiroyuki, S. (2010). Fibrillation of dried chitin into 10–20 nm nanofibers by a simple grinding method under acidic conditions. *Carbohydrate Polymers*, *81*, 134–139.

Sriupayo, J., Supaphol, P., & Rujiravanit, R. (2005). Preparation and characterization of a-chitin whisker-reinforced chitosan nanocomposite films with or without heat treatment. *Carbohydrate Polymers*, *62*, 130–136.

Sikorski, P., Hori, R., & Wada, M. (2009). Revisit of α-chitin crystal structure using high resolution X-ray diffraction data. *Biomacromolecules*, *10*, 1100–1105.